of solution structures of a wide variety of binuclear complexes.

Acknowledgment. We gratefully acknowledge financial support of the Swiss National Science Foundation (Grant 20-28522.90). S.S.M. is grateful to the University of Alexandria for granting him a leave of absence.

Registry No. H_4L^1, 141376-66-1; Cu_2L^1, 141376-71-8; $[Cu_2L^1]\cdot 10H_2O$, 141376-68-3; $[Cu_2L^1]^+$, 141376-72-9; $[Cu_2L^1]^{2+}$, 141376-73-0; L^2, 141376-67-2; $[Cu_2L^2](ClO_4)_4$, 141376-70-7; CuL^3, 133370-41-9; $C_2L^3_2$, 141376-74-1; tetraethyl 1,1,2,2-ethanetetracarboxylate, 632-56-4; ethane-1,2-diamine, 107-15-3.

Supplementary Material Available: Listings of H atom coordinates, thermal parameters, and crystal data for $[Cu_2L^1]\cdot 10H_2O$ and $[Cu_2L^2](ClO_4)_4$ (4 pages); tables of observed and calculated structure factors for the abovementioned compounds (24 pages). Ordering information is given on any current masthead page.

Contribution from the Chemistry Department,
Case Western Reserve University, Cleveland, Ohio 44106

Why the Addition of CO Leads to Acyl Decarbonylation in a Supported Rh Dimer Complex

S.-F. Jen and Alfred B. Anderson*

Received July 30, 1991

Iwasawa and co-workers have recently found that the addition of CO to a Rh dimer complex with an acyl ligand (bound to a silica support) causes decarbonylation accompanied by Rh–Rh bond breaking. Ordinarily decarbonylation occurs in the absence of CO pressure. On the basis of ASED–MO calculations, we find that the driving force for decarbonylation is the stability of the nearly square-planar d^8 Rh that is formed:

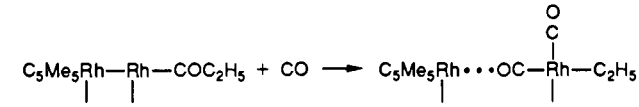

Here the Rh–Rh bond has been cleaved and a CO of the complex on the right forms a weak σ-donation bond with the Rh on the left.

Introduction

It has been known for a while that rhodium monomer complexes have good effectiveness for the hydroformylation reaction in homogeneous systems.[1] The CO insertion reaction is the first step:

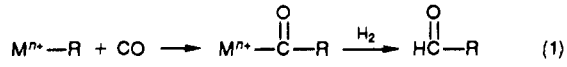

(1)

In general, the CO insertion proceeds under high pressure and the reverse reaction of decarbonylation of the acyl group takes place under vacuum.[1]

Recently, Asakura et al. reported a new aspect of reversible CO insertion on an SiO_2-attached Rh dimer catalyst which showed good catalytic activity for ethene hydroformylation.[2,3] Such heterogeneous catalysts were prepared by the reaction of *trans*-$[Rh(C_5Me_5)(CH_3)]_2(\mu\text{-}CH_2)_2$ with surface OH groups of SiO_2, with C_1 elimination as methane. FTIR spectroscopy showed that the CO insertion into an alkyl group to form acyl proceeds by heating the reaction to 423–473 K under vacuum, while the decarboxylation of the acyl group to form a dicarbonyl and an alkyl occurs under CO pressure at room temperature. On the basis of these findings and EXAFS bond length estimates, the following Scheme I was proposed. In it, the dotted line represents Rh–Rh bond cleavage. The CO pressure dependence observed for this reaction is opposite to that observed for Rh monomer catalysts, for which CO insertion into the metal–alkyl bond is brought about by CO pressure.[1] For the Rh dimer on silica, CO pressure decarbonylates the acyl. The fact that acyl formation was accompanied by Rh–Rh bond formation (2.70 Å bond length) led the authors of ref 2 to suggest that the insertion was in fact being promoted by the metal bond formation. There is little literature

Scheme I

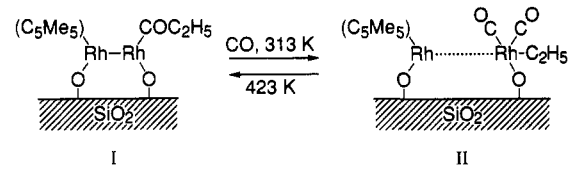

precedence for this idea. A homogeneous CO insertion involving Fe–Fe bond formation has been observed, but it is, unlike the above scheme, irreversible.[4,5]

The purpose of this paper is to undertake a theoretical examination of the electronic structure of species I and II and some potential reaction intermediates to understand the Rh–Rh bond cleavage in the above scheme. The proposed promotion effect of the metal bond formation on the acylation will be investigated.

Method and Models

We have substituted the silica support by hydroxyl groups and also substituted the C_5Me_5 ligand in Rh complexes by C_5H_5(Cp) to simplify the calculations. The choice of hydroxyl groups to represent the silica support is a simplifying approximation since the actual surface structures are not yet established. We have optimized the hydroxyl groups in our calculations because no surface structure information for SiO_2 is available for assigning surface oxygen spacing. We tried fixing the oxygen spacings to be 2.64 and 3.60 Å, respectively, based on spacings in (0001) planes of α-quartz. We found that the calculated structures experienced readjustments in bond angles and lengths and the energies became less stable by up to $^1/_2$ eV when the fixed oxygen spacings were used. Since we do not know what oxygen spacing we should use, we have begun by choosing the optimized ones.

(1) Evans, D.; Osborn, J. A.; Wilkinson, G. *J. Chem. Soc. A* **1968**, 3133.
(2) Asakura, K.; Kitamura-Bando, K.; Isobe, K.; Arakawa, H.; Iwasawa, Y. *J. Am. Chem. Soc.* **1990**, *112*, 3242.
(3) Kitamura-Bando, K.; Asakura, K.; Arakawa, H.; Sugi, Y.; Isobe, K.; Iwasawa, Y. *J. Chem. Soc., Chem. Commun.* **1990**, 253.
(4) Collman, J. P.; Rothrock, R. K.; Finke, R. G.; Rose-Munch, F. *J. Am. Chem. Soc.* **1977**, *99*, 7381.
(5) Collman, J. P.; Rothrock, R. K.; Finke, R. G.; Mooew, E. J.; Rose-Munch, F. *Inorg. Chem.* **1982**, *21*, 146.

0020-1669/92/1331-2651$03.00/0

Table I. Parameters Used in the Calculations: Principal Quantum Number, n; Valence State Ionization Potentials, VSIP (eV); Slater Orbital Exponents, ζ (au); and Linear Coefficients, c for Double-ζ d Orbitals

	s			p			d					
atom	n	VSIP	ζ	n	VSIP	ζ	n	VSIP	c_1	ζ_1	c_2	ζ_2
Rh	5	8.96	2.135	5	5.603	1.835	4	11.06	0.5772	5.542	0.6349	2.098
C	2	15.09	1.608	2	9.76	1.568						
O	2	26.98	2.246	2	12.12	2.227						
H	1	12.1	1.2									

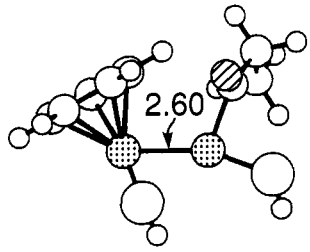

Figure 1. Calculated structure for the surface Rh dimer acyl complex bound to OH groups representing the silica surface, $CpRh{-}RhCOC_2H_5$. The Rh atoms are shaded gray; the O atom bound to C is hatched. The Rh–Rh distance is in Å.

As an additional simplification, the centers of the Cp rings, the Rh, and the OH were all constrained to be in a plane.

The atom superposition and electron delocalization molecular orbital (ASED–MO) theory is used for this study. The details of method are reviewed in ref 6. Parameters used in these calculations are given in Table I. They are based on standard valence orbital exponents[7,8] (ζ) and measured valence state ionization potentials[9] (VSIP) with some adjustments. For rhodium–carbon bonds these were made by studying diatomic RhC: the Rh VSIP was increased and the C VSIP simultaneously decreased in 0.5-eV steps until the calculated charge on C, based on the Mulliken partitioning, approached –0.02, the value estimated from the Pauling electronegativity difference. The final shift was 1.5 eV for the ionization potentials, and no exponent changes were used. This yielded a charge transfer of 0.11 and RhC bond length and strength of 1.88 Å (1.61) and 6.4 eV (6.0) where experimental determinations[10] are in parentheses. The H and O VSIP were assigned the same shifts as C, and the hydroxy oxygen exponents were decreased by 0.2 au, as we do for oxides. Other aspects of the model are as follows. The metal–ligand bond lengths are uncertain by ~0.1 Å; CH bond lengths were overestimated by 0.1 Å, and were optimized to be 1.20 Å for Cp and 1.22 Å for the ethyl group. Cyclopentadienyl was constrained to pentagonal geometry with optimized CC bond lengths which were 1.61 Å for all structures, overestimating actual distance by ~0.15 Å. Since the RhC bond length was overestimated, it may be anticipated that the calculations will also overestimate the equilibrium distance from Rh to the carbonyl ligands.

Results and Discussion

The fully optimized structure of the Rh dimer containing an acyl group is shown in Figure 1. The calculated Rh–Rh bond strength is 2.86 eV for dissociation to unrelaxed fragments; relaxation would lower this bond strength. The correlation of the d^7 Rh fragment orbitals with dimer orbitals is given in Figure 2. The left-hand fragment has a wider dispersion because of the higher Rh coordination number. This leads to its being a donor of one electron to the right-hand Rh fragment, which formally becomes d^8 Rh(I) while the left-hand Rh becomes d^6 Rh(III), and the resulting electron charge-transfer stabilization contributions to the Rh–Rh bond strength, making it stronger than the experimental value for bond order 1. Fragment relaxations would have stabilized the donor orbital, weakening the charge-transfer stabilization. The calculated Rh–Rh distance of 2.60 Å, on the other hand, is reasonable for this bond order and is close to the 2.70 Å EXAFS result from ref 2. The lowest occupied orbital shown on the right-hand side is bonding between Rh and the acyl ligand but has been pushed up in energy due to an antibonding interaction with an O lone-pair orbital. Consequently it has a large d component on the Rh center and participates in the Rh–Rh interaction as shown. However, this orbital does not contribute to the formal d electron count. The high-lying but empty Rh orbital shown on the right-hand side is donated into by the d_z^2-like orbital on the Rh of the left-hand fragment and is responsible for the Rh–Rh σ bond. On the left, two nearly degenerate orbitals, for which energy levels but not orbital pictures are given, are bonding between Rh d orbitals and the occupied Cp e set of orbitals and the top two levels are the antibonding counterparts. The low-lying filled Cp a orbital and high-lying empty e orbitals are just outside the energy range of the figure.

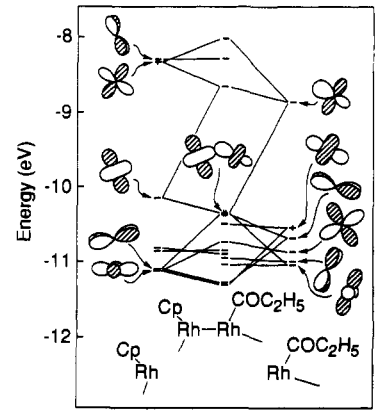

Figure 2. Correlation diagram for metal fragments binding in the acylated Rh dimer complex in the structure of Figure 1.

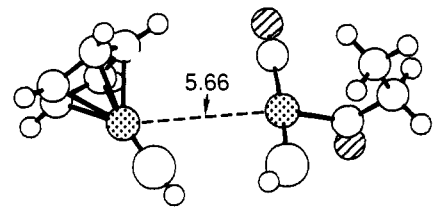

Figure 3. Calculated structure for $CpRh{\cdots}Rh(CO)COC_2H_5$. See caption to Figure 1.

To go from left to right in the reaction scheme, CO attacks the surface dimer complex, and ultimately the Rh–Rh bond is broken. We have studied the bonding of CO to the acylated Rh(I) on the right. We find CO binds strongly, 1.66 eV, and the Rh–Rh bond stretches to 5.66 Å, as shown in Figure 3. This breaking of the bond is a result of the electronic structure of the complex and the σ-donation capability of CO, which pushes the empty orbital on the right-hand fragment (see Figure 2) up in energy and rehybridizes some of the occupied orbitals so that the interaction between the positive fragment on the left and the negative fragment on the right becomes a closed-shell repulsion. This interpretation is shown in Figure 4, which is based on adding CO to the acyl dimer and optimizing the structure while restricting the Rh–Rh distance to 2.60 Å. Again, the lowest occupied orbital of the right-hand fragment in Figure 4 is Rh acyl σ-bonding. Some

(6) (a) Anderson, A. B. *J. Chem. Phys.* **1975**, *62*, 1187. (b) Anderson, A. B.; Grimes, R. W.; Hong, S. Y. *J. Phys. Chem.* **1987**, *91*, 4245.
(7) Basch, H.; Gray, H. B. *Theor. Chim. Acta.* **1966**, *4*, 367.
(8) Clementi, E.; Raimondi, D. L. *J. Chem. Phys.* **1963**, *38*, 2686.
(9) Lotz, W. *J. Opt. Soc. Am.* **1970**, *60*, 206.
(10) Huber, K. P.; Herzberg, G. *Molecular Spectra and Molecular Structure*; Van Nostrand Reinhold Co.: New York, 1978; Vol. 4.

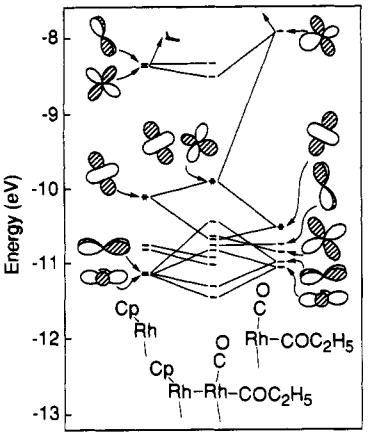

Figure 4. Effects of CO coordination to $CpRh{-}RhCOC_2H_5$ at the right-hand Rh. See caption to Figure 2.

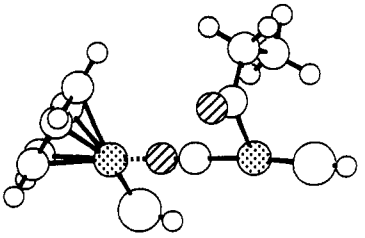

Figure 5. Calculated structure for $CpRhOCRhCOC_2H_5$. See caption to Figure 1.

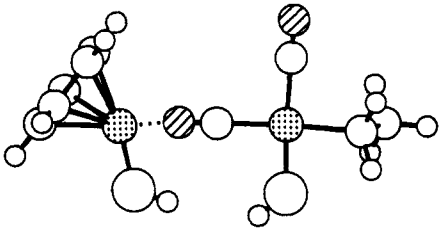

Figure 6. Calculated structure for $CpRhOCRh(CO)C_2H_5$. See caption to Figure 1.

additional stability, 0.92 eV, is calculated by placing the CO colinear with the Rh–Rh axis and reoptimizing the structure, which results in a Rh–Rh distance of 4.82 Å (Figure 5), indicating a σ-bonding stabilization is formed between the O end of the CO ligand and the Rh(III) on the left.

The $CpRhOCRhCOC_2H_5$ intermediate of Figure 5 is calculated to become 0.23 eV more stable when rearranged to the dicarbonyl shown in Figure 6. A planar arrangement of ligand bonds is assumed about the right-hand side d^8 Rh. The four-center Rh···OC-Rh σ bond is due to a net stabilization involving 4σ and 5σ CO-based orbitals in the right-hand fragment by the LUMO of the left-hand fragment. Figure 7 focuses on these interactions. The calculated strength for the Rh···O σ bond is 1.56 eV, based on dissociating into unrelaxed Rh monomer fragments and eliminating the charge transfer stabilization resulting from the half-filled HOMO on the left to the half-filled HOMO on the right. The distance between Rh nuclei is 4.87 Å, which is consistent with the EXAFS result showing no Rh–Rh bonding for this species.

We optimized the $CpRh{-}Rh(CO)_2C_2H_5$ complex in structure II of the reaction scheme (see Figure 8), obtaining a local minimum in the energy, i.e., a metastable structure 2.23 eV less stable than with a bridging CO. As may be seen in Figure 9, there is a single bond between the Rh atoms. Furthermore, the second CO destabilizes a second d orbital on the right and it donates two electrons, so the right-hand Rh becomes d^6 and the left-hand one becomes d^8. The lowest filled orbital shown on the right is the

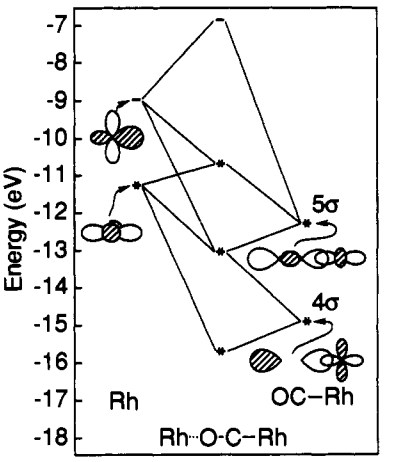

Figure 7. σ interaction between the bridging CO bound to the right-hand Rh fragment and d orbitals on the left-hand fragment.

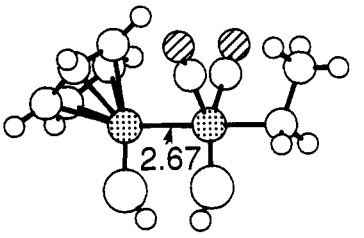

Figure 8. Calculated structure for $CpRh{-}Rh(CO)_2C_2H_5$. See caption to Figure 1.

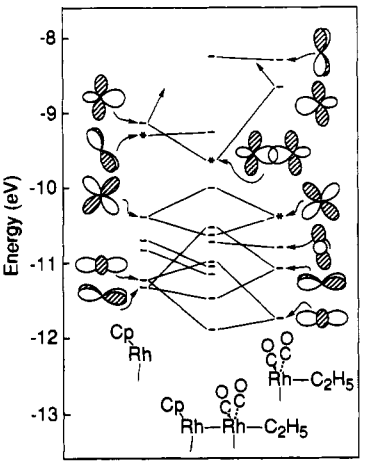

Figure 9. Correlation diagram for metal fragments binding to form $CpRh{-}Rh(CO)_2C_2H_5$ in the structure of Figure 8.

Rh–ethyl σ bond. Given the above results, the electronic structure preference for having the square-planar d^8 Rh(I) on the right and Rh(III) on the left in the complex is 0.67 eV. On the basis of d^8 Rh for the two right-hand fragment structures by themselves, the difference is even greater, 2.58 eV.

Conclusions

The driving force for acylation by this Rh dimer system is not Rh–Rh bond formation because species II of Scheme I would, according to our calculations, also have a Rh–Rh single bond and, again from our rough energy calculations, would be 0.57 eV more stable than the acyl complex with a free CO molecule. Rather than this, species II takes an even more stable structure that is consistent with d^8 Rh on the right, which is square planar with a bridging CO engaged in donation bonding to the left-hand d^6 Rh. This makes species II 2.8 eV more stable than the acyl complex plus gives a free CO molecule. This is a rather large stability and could be overestimated. The largest contribution is for the initial bonding of CO to the acyl complex, 1.66 eV. The

Scheme II

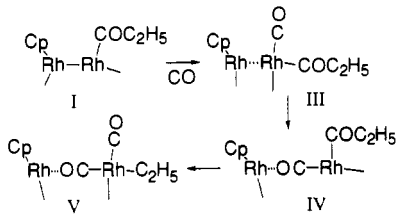

calculated stabilities for all the steps exclude steric and strain instabilities expected on the actual surface.

In place of Scheme I we propose Scheme II. Here CO binds to the acylated Rh fragment on the right to form III. However, the Rh-Rh bond in III is broken so it rearranges to IV with CO nearly colinear with the Rh-Rh axis. Species IV rearranges to V which, like species II that was proposed in ref 2 for Scheme I, has two CO bound to the right-hand Rh, but one of them binds weakly through O to the left-hand Rh. The Rh-Rh distance in II is large, which is consistent with the EXAFS result, and the CO IR spectrum will show splitting as seen in ref 3. The activation energy for the CO insertion reaction, going from V to IV, and its reverse, has not been calculated but, based on a theoretical study involving another low-coordinate transition metal cation,[11] it should be small.

Acknowledgment. We thank the B. F. Goodrich Co. for support of this work through a graduate fellowship.

(11) Anderson, A. B.; Yu, J. *J. Catal.* **1989**, *119*, 135.

Notes

Contribution from the Gross Chemical Laboratory, Duke University, Durham, North Carolina 27706, and Boron Biologicals, Inc., 533 Pylon Drive, Raleigh, North Carolina 27606

A New and Convenient Synthesis of Sodium Carboxylatotrihydroborate, $Na_2BH_3CO_2$, a Boron Analogue of Sodium Acetate

Anup Sood and Bernard F. Spielvogel*

Received May 1, 1990

Acetate ion is a simple yet important species involved in several biological processes,[1] including the biosynthesis of cholesterol. An isoelectronic and isostructural boron analogue of acetate ion is the carboxylatotrihydroborate anion, $H_3BCO_2^{2-}$ (**1**). Thus, **1** may have interesting biological properties due to its structural similarities to the acetate ion. **1** is also isoelectronic with the carbonate ion and is commonly called boranocarbonate.[2] Malone and Parry,[2] while comparing the chemical properties of isoelectronic BH_3CO and CO_2, synthesized several salts of **1** by reaction of H_3BCO with alcoholic base. They also showed that H_3BCO can be regenerated from salts of **1** by reaction with 85% H_3PO_4. Use of H_3BCO as an acyl ion equivalent has been demonstrated previously,[3,4] and provides a convenient route for incorporating boron into molecules with easy to acylate functionalities. The resulting species may have potential in boron neutron capture therapy (BNCT). Since salts of **1** are stable for long periods under ambient conditions, these should be convenient solid storage sources for the generation of BH_3CO upon demand. In addition, they may also be of value as selective reducing agents[4] (such as found for cyanoborohydride).

Despite the potential use of **1**, studies of the chemistry and biological activity of this species have been limited due in part to the hazardous nature of its synthesis. The previous synthesis,[2] as mentioned (vide supra), involved the use of H_3BCO, which itself is prepared from B_2H_6 and CO under pressure. Not only are all these gases hazardous, but the synthesis also requires use of special equipment. We now wish to report a new and convenient synthesis of sodium boranocarbonate and the results of preliminary studies of its biological activity.

Reaction of the sodium salt[5] of trimethylamine-carboxyborane[6] (**2**) with 2 molar equiv of sodium diethyldihydroaluminate (Aldrich) in refluxing THF yielded **1** in ca. 50% yield[7] according to Scheme I. The product was easily isolated by filtration under an inert atmosphere. The major byproduct was the completely

Scheme I

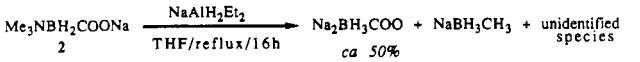

Scheme II

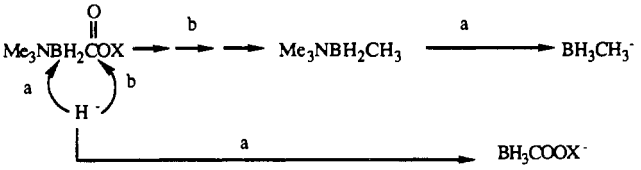

reduced species $NaBH_3CH_3$, which stayed in solution with small amounts of other unknown byproducts. At least 1.5 molar equiv of reagent was necessary to completely consume the starting material under the conditions reported. With lower amounts of reagent (1.0-1.25 equiv), a small amount of unreacted starting material contaminated the product without increasing the yield (by decreasing the amount of reduction). Free trimethylamine-carboxyborane could also be used as substrate, but it consumed extra valuable reagent by immediate conversion to salt.

Attempts to prepare *O*-methylboranocarbonate, $H_3BC(O)OMe^-$, from trimethylamine-carbomethoxyborane,[8] $Me_3NBH_2CO_2Me$, by a similar procedure were unsuccessful; instead formation of $BH_3CH_3^-$ was observed. Reaction[9] of Me_3NBH_2COOX (X = H, Na, Me) with several other hydrides (except NaH) either gave no reaction or formed $M^+BH_3CH_3^-$ and/or $Me_3NBH_2CH_3$ (Table I). This itself is a new method for the preparation of $M^+BH_3CH_3^-$ and has been utilized for the

* To whom correspondence should be addressed at Boron Biologicals, Inc.

(1) Lehninger, A. L. *Biochemistry*; Worth Publishers Inc.: New York, 1975.
(2) Malone, L. J.; Parry, R. W. *Inorg. Chem.* **1967**, *6*, 817-822.
(3) Zetlmeist, M. J.; Malone, L. J. *Inorg. Chem.* **1972**, *11*, 1245-1247 and references therein.
(4) Spielvogel, B. F.; McPhail, A. T.; Knight, J. A.; Moreland, C. G.; Gatchell, C. L.; Morse, K. W. *Polyhedron* **1983**, *2*, 1345-1352.
(5) **2** was prepared in 97% yield by reaction of Me_3NBH_2COOH with $NaHCO_3$ using a procedure similar to the one reported by Morse et al. (Norwood, V. M., III; Morse, K. W. *Inorg. Chem.* **1986**, *25*, 3690-3693). ^1H NMR: 2.60 ppm, s. ^{11}B NMR: -8.00 ppm, t, $^1J_{B,H}$ = 94 ● 1 Hz.
(6) Spielvogel, B. F.; Wojnowich, L.; Das, M. K.; McPhail, A. T.; Hargrave, K. D. *J. Am. Chem. Soc.* **1976**, *98*, 5702-5703.
(7) Yields up to 66% have been obtained. ^1H NMR: 0.73 ppm, q, $^1J_{^{11}B,H}$ = 80 ± 1 Hz, and septet, $^1J_{^{10}B,H}$ = 26.7 ± 0.21 Hz. ^{11}B NMR: -31.1 ppm, q, $^1J_{^{11}B,H}$ = 80 ± 2 Hz. Anal. Calcd for $BH_3CO_2Na_2$: C, 11.57; H, 2.91; B, 10.41. Found: C, 11.26; H, 2.92; B, 9.79.
(8) Spielvogel, B. F.; Ahmed, F. V.; McPhail, A. T. *Synthesis* **1986**, 833-835.
(9) The reactions were followed by ^{11}B NMR spectroscopy.

0020-1669/92/1331-2654$03.00/0